Am J Cancer Res 2019;9(8):1664-1681
www.ajcr.us /ISSN:2156-6976/ajcr0095398

Original Article

Tannic acid attenuates the formation of cancer stem cells by inhibiting NF-κB-mediated phenotype transition of breast cancer cells

Dal-Ah Kim[1,2], Hack Sun Choi[1,2], Eun-Sun Ryu[1,2], Jiyeon Ko[1,2], Hyun-Soo Shin[1,2], Jong-Min Lee[1,2], Heesung Chung[3], Eunsung Jun[4,5], Eok-Soo Oh[3], Duk-Hee Kang[1,2]

[1]The Department of Internal Medicine, [2]Ewha Medical Research Center, College of Medicine, Ewha Womans University, Seoul 07804, Republic of Korea; [3]Department of Life Science, The Research Center for Cellular Homeostasis, Ewha Womans University, Seoul 03760, Republic of Korea; [4]Division of Hepato-Biliary and Pancreatic Surgery, Department of Surgery, University of Ulsan College of Medicine, Asan Medical Center, Seoul, Republic of Korea; [5]Department of Convergence Medicine, Asan Institute for Life Sciences, University of Ulsan College of Medicine, Seoul 05505, Republic of Korea

Received April 14, 2019; Accepted June 28, 2019; Epub August 1, 2019; Published August 15, 2019

Abstract: Cancer stem cells (CSCs) are innately resistant to standard therapies, which positions CSCs in the focus of anti-cancer research. In this study, we investigated the potential inhibitory effect of tannic acid (TA) on CSCs. Our data demonstrated that TA (10 μM), at the concentration not inhibiting the proliferation of normal mammary cells (MCF10A), inhibited the formation and growth of mammosphere in MCF7, T47D, MDA-MB-231 cells shown as a decrease in mammosphere formation efficiency (MFE), cell number, diameter of mammosphere, and ALDH1 activity. NF-κB pathway was activated in the mammosphere indicated by an up-regulation of p65, a degradation of IκBα, and an increased IL-6. The inhibition of NF-κB pathway via gene silencing of p65 (sip65), NF-κB inhibitor (PDTC), or IKK inhibitor (Bay11-7082) alleviated MFE. Other CSCs markers such as an increase in ALDH1 and $CD44^{high}$/$CD24^{low}$ ratio were ameliorated by sip65. TA also alleviated TGFβ-induced EMT, increase in MFE, and NF-κB activation. In murine xenograft model, TA reduced tumor volume which was associated with a decrease in $CD44^{high}$/$CD24^{low}$ expression and IKK phosphorylation. These results suggest that TA negatively regulates CSCs by inhibiting NF-κB activation and thereby prevents cancer cells from undergoing EMT and CSCs formation, and may thus be a promising therapy targeting CSCs.

Keywords: Tannic acid, EMT, cancer stem cells, mammosphere, NF-κB signaling

Introduction

Breast cancer is one of most prevalent female cancers, and also a leading cause of cancer-associated death in women [1]. Although conventional therapies such as surgery, chemotherapy, and hormone therapy have improved the survival rate among patients with breast cancer, disease recurrence and metastasis remain as significant problems [2, 3]. Cancer stem cells (CSCs) are a subset of cancer cells that have the ability to self-renew [4-6], and are regarded as being responsible for tumor initiation and resistance to chemotherapy, thereby ultimately causing tumor metastasis and disease relapse [7, 8]. Accordingly, many studies to date have focused on the development of effective therapies targeting CSCs [9, 10].

Nuclear factor kappa-light-chain-enhancer of activated B cells (NF-κB)-family transcription factors are well established to both play key roles in cell survival, proliferation, inflammation, tumor invasion, and metastasis, and to be overexpressed or activated in breast-cancer cell lines and primary human breast-tumor cells [11, 12]. In addition, suppressing NF-κB signaling has been shown to decrease the $CD44^{high}$/$CD24^{low}$ cell population, reduce stem cell expansion, and repress the Nanog and Sox2 expression in a Her2-driven murine model of breast cancer [13, 14], suggesting that NF-κB signaling may critically mediate the behavior of breast CSCs.

The epithelial-mesenchymal transition (EMT) has been shown to be an early mechanism for

cancer invasion and metastasis [15, 16]. Morel et al. previously reported that human mammary epithelial cells undergoing EMT exhibited an increase in stem-like capability [17]. In fact, the EMT has been shown to enable cancer cells to acquire stem cell-like properties via the effects on a range of key signaling pathways associated with cancer-cell metastasis and drug resistance, including the TGFβ, Notch, Wnt, AKT-mTOR, MAPK/ERK, and NF-κB pathways [18-23].

A previous study conducted by our group screened a range of natural compounds using a medium-throughput automated mammosphere counting method [24], and resultantly revealed that tannic acid (TA) exerted a substantial inhibitory effect on the formation of breast CSCs. TA (C76H52046) is a specific type of water-soluble polyphenol tannin whose structure consists of numerous phenolic rings. TA is known to be a strong anti-oxidant that prevents reactive oxygen species (ROS)-mediated drug toxicity [25] by scavenging free and superoxide radicals [26]. Similar to other polyphenols, TA has been shown to induce the apoptosis, and inhibit the proliferation of various cancer cells [27-30]. Additionally, TA treatment has been demonstrated to inhibit the potent anti-angiogenic factor CXCL12/CXCR4 in breast-cancer cells, again suggesting it as a promising therapeutic target for the disease [31]. However, to date, the effect of TA on breast CSCs has not yet been investigated.

Thus, the present study analyzed the effects of TA on the formation and growth of breast CSCs, and also assessed the mechanisms underlying these effects in cultured breast cancer cells and *in-vivo* mouse xenograft model of breast cancer.

Materials and methods

Reagents

All chemicals and tissue plates were obtained from MilliporeSigma (Burlington, MA, USA) or Nunc Labware (Waltham, MA, USA), unless otherwise stated.

Cell culture

Human normal breast cells (MCF10A) and the human breast cancer cells (MCF7, T47D and MDA-MB-231) were purchased from ATCC (Manassas, VA, USA). The MCF10A cells were maintained (37°C, in a humidified incubator with 5% CO_2) in DMEM/F12 culture medium (Thermo Fisher Scientific, Waltham, MA, USA) that was supplemented with 10% fetal bovine serum (FBS; Hyclone Laboratories, Logan, UT, USA), 20 ng/mL EGF, 0.5 mg/mL hydrocortisone, 100 ng/mL cholera toxin, 10 μg/mL insulin, and 100 U/mL penicillin. Likewise, the MCF7 cells were maintained in DMEM culture medium (Hyclone Laboratories) and the T47D, MDA-MB-231 cells were maintained in RPMI-1640 medium (Hyclone Laboratories) that was supplemented with 10% FBS, 100 U/mL penicillin, and 100 μg/mL streptomycin (Hyclone Laboratories).

Cell proliferation and cytotoxicity assays

To determine TA concentration at which the viability of normal breast cells was maintained, the effect of TA treatment (0-100 μM) on the viability of both normal breast epithelial cells (MCF10A) and breast-cancer cells (MCF7) was compared to that of paclitaxel, which is one of the most commonly prescribed chemotherapeutic agents in breast cancer [32]. Cell proliferation was assessed using a 3-(4,5-dimethylthiazol-2-yl)-5-(3-carboxymethoxy phenyl)-2-(4-sulfophenyl)-2H-tetra-zolium (MTS) uptake assay (Promega, Madison, WI, USA) as previously described [33]. MCF7/MCF10A cytotoxicity after TA or paclitaxel treatment (48 h) was determined by measuring the amount of lactate dehydrogenase (LDH) that was released into the medium using the LDH cytotoxicity detection kit (Roche Diagnostics, Mannheim, Germany). Treatment with up to 20 μM TA did not affect the viability nor proliferation of the MCF10A cells over the 48-h (Figure S1), whereas in contrast, treatment with a paclitaxel concentration greater than 5 nM was shown to significantly increase LDH release by the MCF10A cells (Figure S2). Therefore, TA concentrations of 10 and 20 μM were selected for use and comparison with 5 nM of paclitaxel in the subsequent *in-vitro* experiments.

Mammosphere assays

During the sphere assay, cells (MCF7, 4×10^4 cells/well; T47D, 2×10^4 cells/well; MDA-MB-231, 5×10^3 cells/well) were seeded in ultra-low attachment 6-well plates and main-

tained (37°C, 5% CO_2) in 2 ml of complete MammoCult™ medium (StemCell Technologies, Vancouver, BC, Canada) that was supplemented with 4 μg/mL heparin, 0.48 μg/mL hydrocortisone, 100 U/mL penicillin, and 100 μg/mL streptomycin. After 7 days, all primary spheres of 50-120 μm in diameter were counted. To establish secondary and tertiary mammospheres, these primary mammospheres were harvested and pipette-mixed with 1X Trypsin/EDTA to form a single cell suspension, before being plated once again using the same conditions, and grown for 5 days [34]. Automated counting of mammospheres with a diameter > 50 μm was achieved by using the NICE software program to analyze scanned images that were captured using NIS-Elements BR 4.4 software (Nikon, Tokyo, Japan), as previously described [24]. The observed mammosphere-formation efficiency (MFE, %) was calculated to be the (number of spheres per well/number of MCF7 cells seeded per well) × 100.

Western blot analysis

The cells were lysed in 1X RIPA buffer containing a protease inhibitor mixture. Nuclear extracts were isolated using a Nuclear extraction kit (Promega). The resolved proteins were then transferred to a polyvinylidine difluoride (PVDF) membrane (MilliporeSigma). The membranes were blocked (30 min, room temperature) in 3% bovine serum albumin (BSA) in PBS-Tween 20 (0.1%, v/v), and then incubated (overnight, 4°C) with primary antibodies against E-cadherin, N-cadherin, Fibronectin (BD Biosciences, San Jose, CA, USA), p-IκBα, IκBα, CD44, pIKK, IKK (Cell Signaling Technology, Danvers, MA, USA), cytokeratin-18 (CK18), Vimentin, CD24, IL-6, ALDH1, p65, LaminB and β-actin (Santa Cruz Biotechnology, Dallas, TX, USA). After washing with 0.1% PBS-Tween 20, the blots were incubated with appropriate horseradish peroxidase (HRP)-conjugated secondary antibodies, and the resulting signal was detected using an enhanced chemiluminescence detection system (Santa Cruz Biotechnology). The intensity of each band was determined by densitometry using ImageJ software (National Institutes of Health, Bethesda, MD, USA; http://imagej.nih.gov/ij).

Immunofluorescent staining of MCF7 cells

The MCF7 cells were seeded in 6-well plates containing coverslips, and treated (48 h) with TGFβ (10 ng/mL) and/or TA (10 μM). The cells were then fixed (5 min) with 3.7% paraformaldehyde, permeabilized (3 min) with 1% triton X-100 in PBS, blocked (30 min) with 1% BSA, and incubated (overnight, 4°C) with the mouse anti-E-cadherin antibody (1:200; BD Bioscience). After washing with PBS, the cells were incubated (1 h, room temperature) with Alexa-588 conjugated goat anti-mouse antibody (1:200; Thermo Fisher Scientific), and mounted on slides using mounting solution containing 4',6-diamidino-2-phenylindole (DAPI) (Vector Laboratories, Burlingame, CA, USA). Images were captured using a fluorescence microscope (Carl Zeiss GmbH, Oberkochen, Germany).

Extraction of total RNA and real-time PCR

Total RNA was extracted using RNeasy Mini Kit (Qiagen, Hilden, Germany), according to the manufacturer's protocol. The DNA-free RNA was reverse-transcribed into cDNA using the Superscript First Strand Synthesis system (MilliporeSigma). Real-time PCR was performed on the ABI PRISM 7000 Sequence Detection system using SYBR Green I as a double-stranded DNA-specific dye according to the manufacturer's instructions (Thermo Fisher Scientific). The PCR reaction was performed with 1 μL of cDNA, 10 μL of SYBR Green PCR master mix (Thermo Fisher Scientific), and 10 pM of sense and antisense primers of E-cadherin (forward primer: 5'-ACCCCTGTTGGTGTCTTT-3', reverse primer: 5'-TTCGGGCTTGTTGTCATTCT-3'), CK18 (forward primer: 5'-TCTCTGAGGCTGCCAACCG-3', reverse primer: 5'-CGAAGGTGACGAGCC-ATTTCC-3'), N-cadherin (forward primer: 5'-CGAGCCGCCTGCGCTGCCAC-3', reverse primer: 5'-CGCTGCTCTCCGCTCCCCGC-3'), Fibronectin (forward primer: 5'-GGGAACGGAAAAGGAGAA-3', reverse primer: 5'-AGCAAATGGCACCGAGA-TA-3'), and β-actin (forward primer: 5'-TTC-TGACCCATGCCCACCAT-3', reverse primer: 5'-ATGGATGATATCGCCGCGCTC-3') for a final volume of 20 μL per reaction. Optimal primer concentrations were determined by preliminary experiments. The PCR cycle conditions for human gene consisted of 95°C for 60 seconds, 55°C for 30 seconds, and 60°C for 45 seconds followed by a 10 minutes extension at 72°C (40 cycles). All PCR procedures were replicated at least three times. The amount of PCR products was normalized with the housekeeping gene, β-actin, to determine the relative expression ratios for each mRNA to the control group.

Aldehyde dehydrogenase (ALDH) activity

ALDH activity was measured using a commercial ALDEFLUOR™ Kit (STEMCELL Technologies). The cells were treated with TA (24 h), and then incubated (30 min, 37°C) with the ALDEFLUOR substrate. The ALDH1 inhibitor, diethyl-aminobenzaldehyde (DEAB) was used as a negative control to define the ALDEFLUOR-positive region. Control and treated samples were analyzed using the Acuri C6 flow cytometer (BD Bioscience).

Electrophoretic mobility shift assay (EMSA)

Double-stranded oligonucleotide DNA containing the NF-kappa B binding site (5'-AGTTGAGGGGACTTTCCCAGGC-3' and 5'-GCCTGGGAAAGTCCCCTCAACT-3') were annealed, and the resulting double-stranded oligonucleotides then end-labeled with [γ-^{32}P] dATP. Free nucleotides were separated via centrifugation through a G-25 column (Roche Diagnostics). The end-labeled DNA probes were incubated (20 min, room temperature) with *nuclear extracts* in a final volume of 20 μl EMSA buffer (comprising 10 mM Tris pH 7.5, 5% glycerol, 1 mM EDTA pH 7.1, 50 mM NaCl, 1 mM DTT, and 0.1 mg/ml poly [dI-dC]). The resulting reaction mixtures were separated via electrophoresis (4°C) on a 4% polyacrylamide non-denaturing gel in 0.5XTBE (45 mM Tris borate and 1 mM EDTA), and visualized via autoradiography.

Small interfering RNA (siRNA)

A non-specific control siRNA, and a siRNA targeting human *p65* mRNA (NM_021975.2), were purchased from Bioneer (Daejeon, Korea). Cells were then seeded on 6-well plates and grown (24 h) in cultured medium supplemented with 10% FBS, before being transfected with the *p65* siRNA using Lipofectamine® RNAiMAX (Thermo Fisher Scientific) according to the manufacturer's instructions. After 48 h, the cells were subjected to a western-blot analysis.

Mouse xenograft tumor model

Han's method [20] for generating a subcutaneous (SQ) xenograft mouse model was modified for the present study. Briefly, 1.5 × 10^7 MCF7 cells were suspended in a 1:1 mixture of PBS and matrigel, and this was implanted in 6-week-old female Balb/c nude mice (Nu/Nu, Orient Bio Inc., Seongnam, Korea) via SQ injection into the right flank. The mice were assigned to either a control (N = 5), TGFβ (N = 5), or TGFβ + TA (N = 6) group. Mice in the latter two groups received an intraperitoneal injection of TGFβ (40 ng/kg) three times/wk for 4 wks to facilitate tumor growth as reported [20], and those in the third group also received an intraperitoneal injection of TA (2 mg/kg) twice/wk (on alternative days to the TGFβ injection). Tumor growth was measured using a caliper, and tumor volume was calculated using the following formula: $V = (d^2 \times D)/2$, where d is the smallest diameter, and D is the largest diameter of the tumor. All animal experiments and procedures were conducted in strict accordance with a protocol approved by the Institutional Animal Care and Use Committee (IACUC) of the Ewha Woman's University (ESM 16-0343).

Immunohistochemistry (IHC) of breast tumor tissue

Tumor tissues isolated from xenograft were fixed (overnight) in 4% formalin, and paraffin-embedded tissue sections (5 μm) were deparaffinized and rehydrated with xylene and ethanol, respectively. Section slides were boiled (30 min, 100°C) in citrate buffer (pH 6.0) to facilitate antigen retrieval, and then blocked firstly (10 min, room temperature) in 3% H_2O_2 in methanol, and subsequently with 3% BSA (30min, room temperature). They were then incubated (overnight, 4°C) with an anti-CD44 monoclonal antibody (1:200; Cell signaling), followed by an incubation with a biotinylated anti-mouse IgG secondary antibody (1:200; Vector Laboratories) for 1 h at room temperature. The resulting signals were detected via application of the ABC reagent (Vector Laboratories) and diaminobenzidine (DAB), before the tissues were hematoxylin counterstained, and analyzed.

Statistical analysis

All statistical analyses were conducted using GraphPad Prism version 5.0. (GraphPad Software, La Jolla, CA, USA). Data were presented as means ± SE. A student's t test was used to compare the mean values of two independent groups. A parametric one-way ANOVA and a non-parametric Kruskal-Wallis test were used to assess statistical differences between more than two groups. A *p-value < 0.05 was considered* to indicate statistical significance.

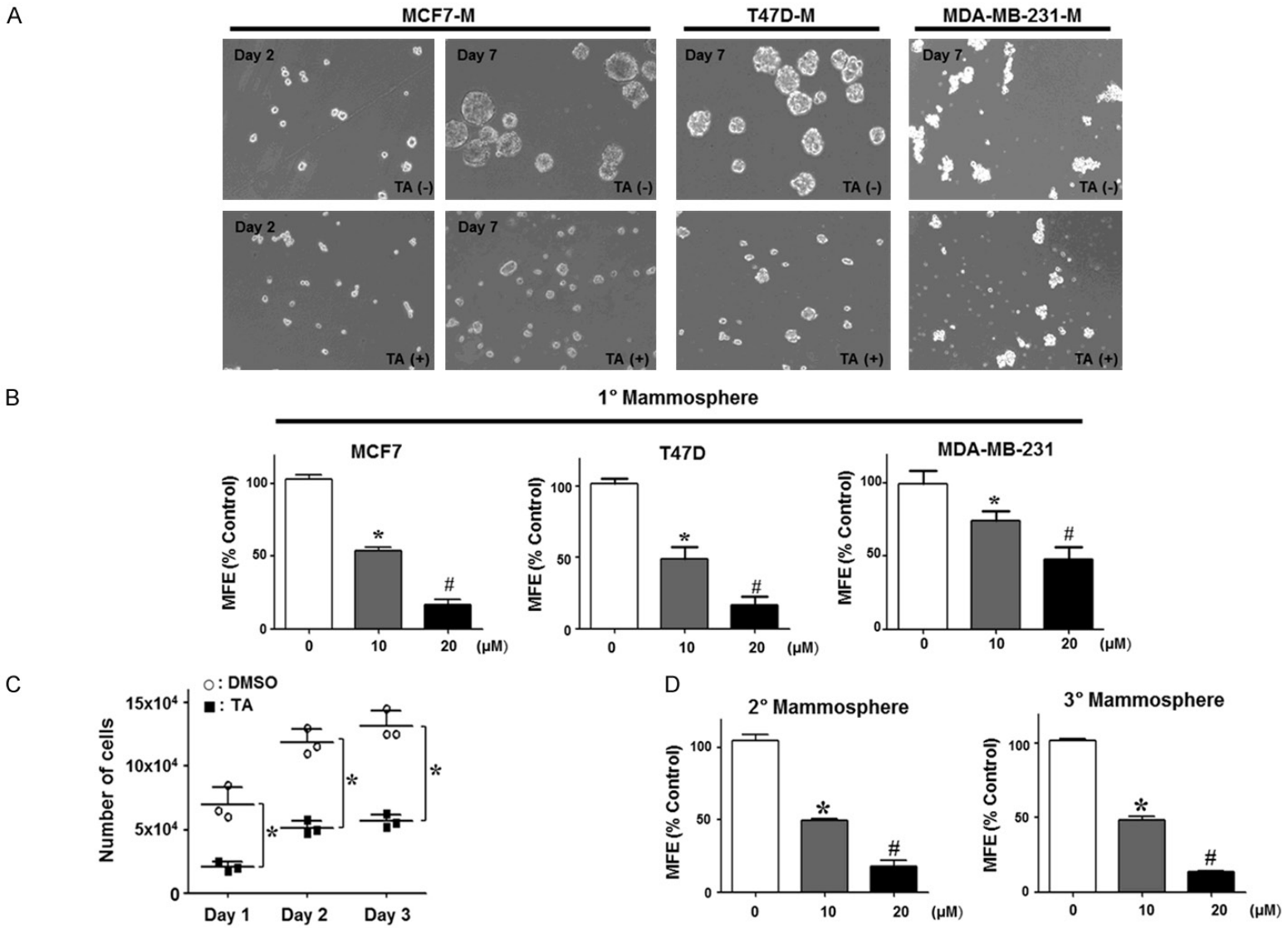
A
MCF7-M
T47D-M
MDA-MB-231-M
Day 2
Day 7
TA (-)
TA (+)
B
1° Mammosphere
MCF7
T47D
MDA-MB-231
MFE (% Control)
100
50
0
*
#
0
10
20
(μM)
C
○: DMSO
■: TA
Number of cells
15x10⁴
10x10⁴
5x10⁴
0
Day 1
Day 2
Day 3
D
2° Mammosphere
3° Mammosphere

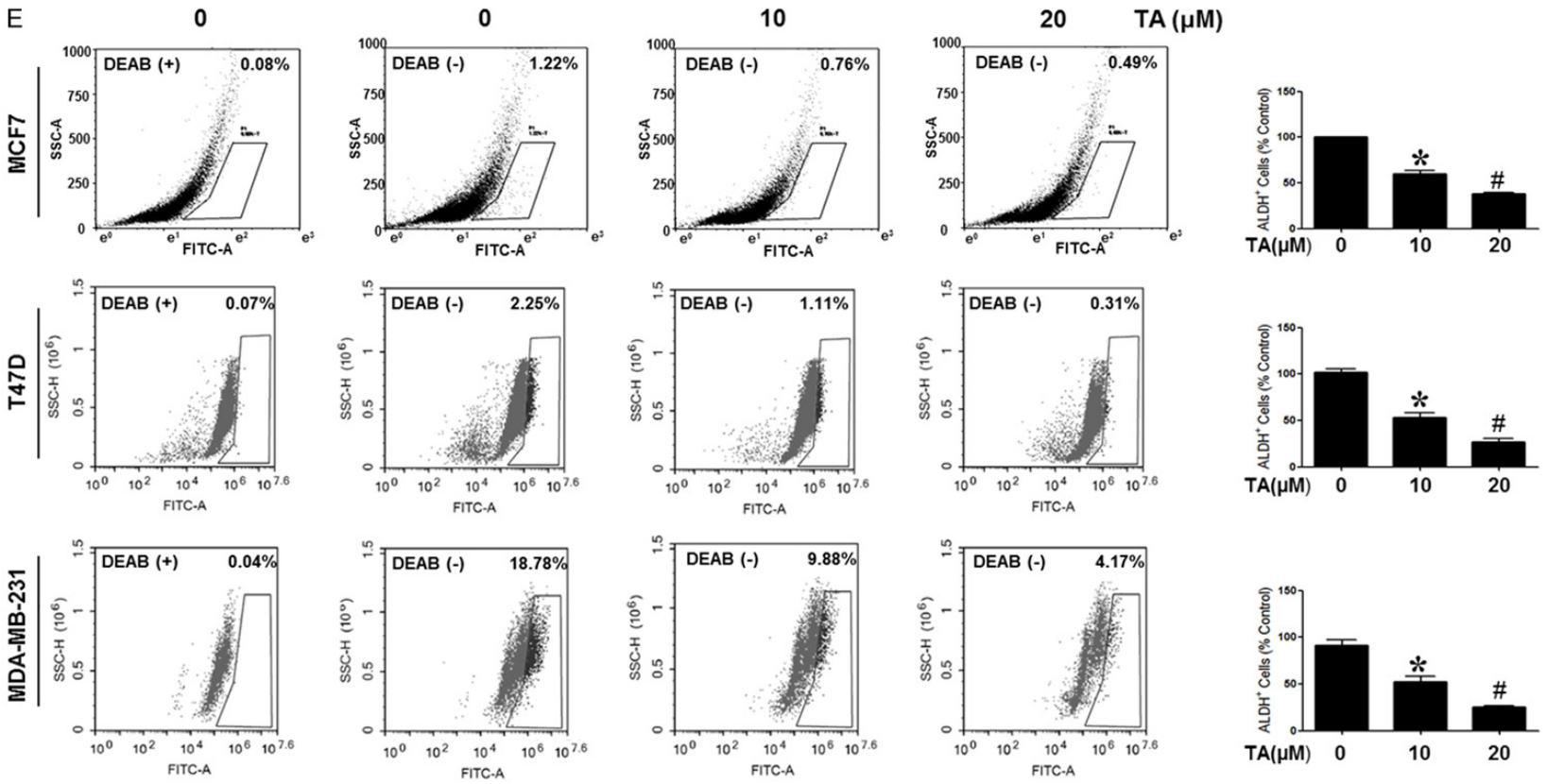

Figure 1. TA reduces the mammosphere forming ability of breast cancer cells. A. Spheres derived from a single-cell suspension of MCF7, T47D, and MDA-MB-231 cells were visible after 7 days of culture with complete MammoCult™ medium. Treatment with TA (10 μM) resulted in a significant decrease in the diameter of the produced mammospheres. Magnification, × 200. B. Treatment with TA (10 and 20 μM) reduced the mammosphere formation efficiency (MFE) in cells assessed by using NICE software to count the number of spheres with a diameter > 50 μm, after histogram pitting. C. Treatment of mammospheres for 2-3 days with TA (10 μM) significantly decreased their number of constituent cells compared to treatment with DMSO. Cells were counted in triplicate, and the mean ± SEM plotted. D. The inhibitory effect of TA (10 and 20 μM) on the MFE was also observed in secondary and tertiary mammosphere assays. Representative images of tumor spheres with quantitation bars are shown. E. The proportion of ALDH-positive cells as quantified via an ALDEFLUOR assay was significantly decreased after TA treatment (10 and 20 μM). The upper and lower panels show representative dot blots, in which ALDH-positive cells were treated with (upper) or without (lower) the ALDH inhibitor, DEAB. Values in dot plots indicate the percentage of ALDH-positive cells within a population. The data on the quantitation bar graph are the mean ± SEM of three independent experiments. *$P < 0.05$ vs. control; #$P < 0.05$ vs. 10 μM of TA.

Results

TA reduces the CSC formation of breast cancer cells

As the first step toward understanding whether TA regulates the stemness of breast cancer, the effect of TA on breast CSCs was assessed by analyzing mammosphere formation and growth in two luminal breast cancer cell lines (MCF7 and T47D cells) and triple-negative breast cancer cell line (MDA-MB-231 cells). The TA-treated cells exhibited a reduced diameter of mammosphere (**Figure 1A**) and MFE in a dose-dependent manner (**Figure 1B**), indicating that TA inhibited the formation of mammospheres (MCF7-M, T47D-M, and MDA-MB-231-M) derived from MCF7, T47D, and MDA-MB-231, respectively. In addition, TA treatment significantly reduced the number of constituent cells of MCF7-M (**Figure 1C**). When we compared the effect of TA (10 μM) with paclitaxel, the most commonly prescribed medicine for breast cancer, this inhibitory effect of TA (10 μM) on the MFE in MCF7 cells was greater than that which was achieved using paclitaxel (5 nM) at the concentrations which did not affect cell viability (Figures S1, S2). Furthermore, the inhibitory effect of TA on sphere formation was observed in secondary and tertiary mammosphere assays (**Figure 1D**). The effect of TA on CSC ALDH activity was assessed by using an ALDEFLOUR assay to determine the proportion of ALDH-positive breast-cancer cells, which is regarded as another marker of tumor stemness [8]. TA (10 and 20 μM) for 24 hours decreased the proportion of ALDH-positive breast-cancer cells in a dose-dependent manner (**Figure 1E**).

TA blocks the NF-κB pathway in the mammospheres derived from MCF7, T47D, and MDA-MB-231 cells

Given the known association between CSC formation and NF-κB pathway activation [35, 36], the effect of TA treatment on NF-κB signaling in breast CSCs was next examined. The expression of p65 was found to be increased in the MCF7-M, T47D-M, and MDA-MB-231-M compared to MCF7, T47D, and MDA-MB-231 with a reduction in IκBα expression. (**Figure 2A**). TA treatment both dose-dependently reduced the nuclear p65 expression (**Figure 2B**), and reversed the IκBα degradation exhibited by MCF7-M, T47D-M and MDA-MB-231-M (**Figure 2C**). TA also decreased the nuclear p65 DNA binding in MCF7-M, as revealed via EMSA which utilized a P^{32}-labeled p65 probe (**Figure 2D**). The levels of IL-6, which is one of the most highly induced NF-κB-dependent cytokines [37], were also increased in MCF7-M compared to the MCF7 cells, which was significantly inhibited by TA (**Figure 2E**, **2F**). These findings suggest that NF-κB/IL-6 signaling is activated in breast CSCs, and that this activation is inhibited by treatment with TA.

Inhibition of NF-κB signaling decreases the formation of breast CSCs

To verify the role of NF-κB signaling in the formation of breast CSCs, we investigated the effect of specific gene silencing or corresponding inhibitors of the components of NF-κB pathway. siRNA-induced silencing of *p65* expression was shown to reduce the formation of mammosphere in MCF7, T47D, and MDA-MB-231 cells (**Figure 3A**). As shown in **Figure 3B** and **3C**, treatment with either PDTC (a NF-κB pathway-specific inhibitor) or BAY 11-7082 (an irreversible inhibitor of IKK) resulted in a significant decrease in the formation of mammosphere expressed as a decrease in MFE from the concentration of 5 μM and 2 μM, respectively (**Figure 3B** and **3C**). *p65* silencing also reduced the expression of ALDH1, and the exhibited $CD44^{high}/CD24^{low}$ ratio (**Figure 3D**). These findings suggest that NF-κB signaling critically regulate CSC formation in breast cancer.

TA reduces TGFβ-induced EMT and CSC formation in MCF7 and T47D cells

Since the EMT is regarded as a key process required for CSC formation [21], the effect of TA treatment on TGFβ-induced EMT in MCF7 cells was next assessed. TGFβ is a representative cytokine known to enhance the 'stemness' of tumor cells [38, 39]. In the present study, TGF-β (10 ng/mL) induced EMT of MCF7 and T47D, as indicated by morphologic transition from cuboidal cells to elongated mesenchymal phenotype with a loss of cell-to-cell contact (**Figure 4A**). In parallel, this morphologic transition was accompanied with a decreased expression of epithelial cell markers (E-cadherin and CK18) and an increased expression of mesenchymal cell markers such as N-cadherin and fibronectin (**Figure 4B-D**). Notably, TA treatment (10 μM) alleviated TGFβ-induced EMT, demonstrated as a reversal of cell morphology and altered

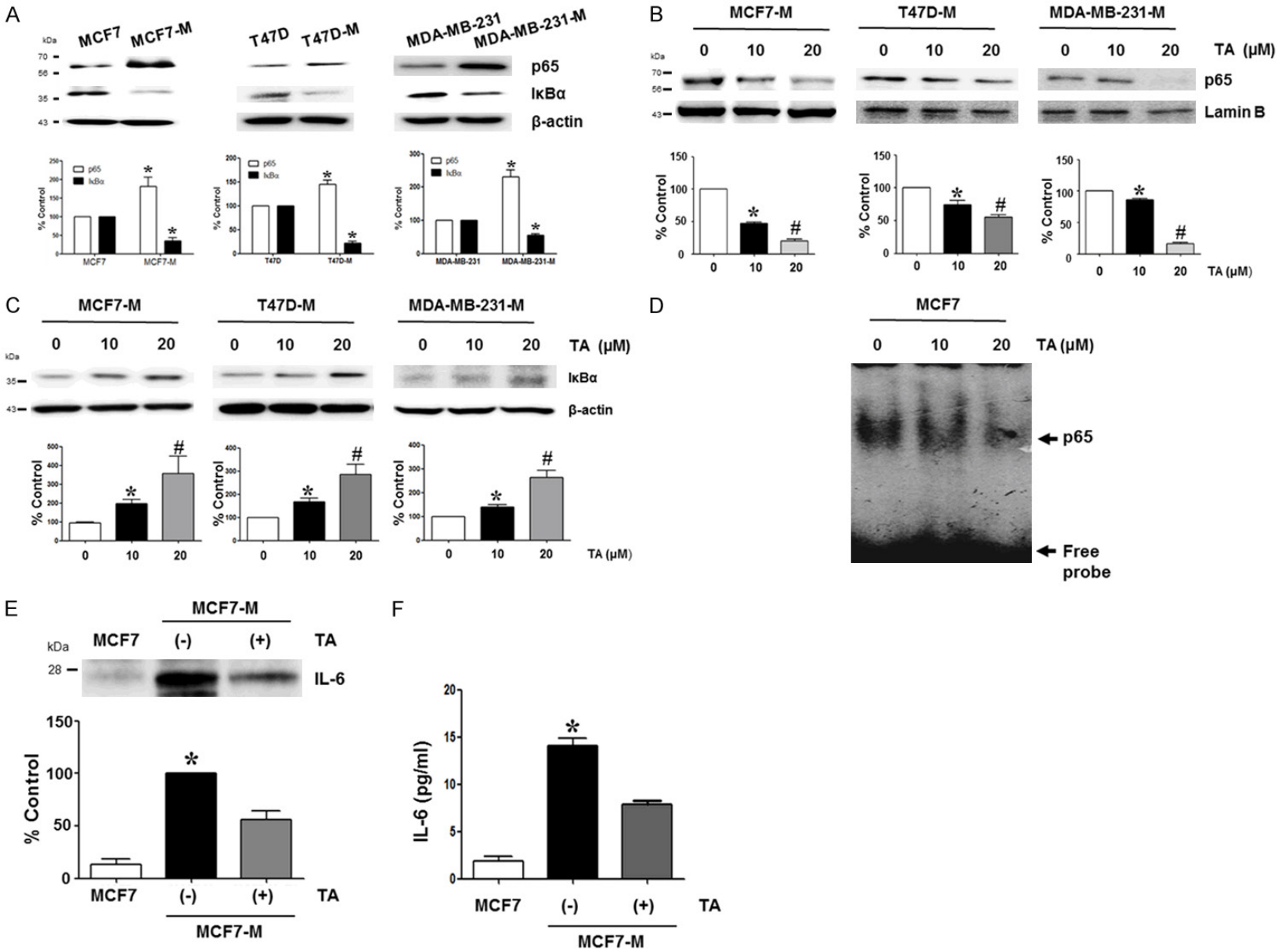
A
MCF7
MCF7-M
T47D
T47D-M
MDA-MB-231
MDA-MB-231-M
p65
IκBα
β-actin
% Control
B
MCF7-M
T47D-M
MDA-MB-231-M
TA (μM)
Lamin B
C
IκBα
β-actin
D
MCF7
p65
Free probe
E
MCF7-M
TA
IL-6
F
IL-6 (pg/ml)

Figure 2. TA blocks the NF-κB pathway activation in mammospheres. (A) p65 expression was increased in the breast cancer cell-derived mammosphere (MCF7-M, T47D-M, and MDA-MB-231-M) compared to the breast cancer cells (MCF7, T47D, and MDA-MB-231) whereas IκBα expression was decreased in MCF7-M, T47D-M, and MDA-MB-231-M. (B, C) TA treatment (10 μM) decreased the p65 expression in the nuclear protein extracted from the breast cancer cell-derived mammosphere (B), and also blocked IκBα degradation in a dose-dependent manner (C). β-actin and Lamin B were used as loading controls for the whole-cell and nuclear protein extracts, respectively. (D) TA treatment (10 μM) decreased the DNA/p65 interaction in the mammospheres. A presentative EMSA assay using nuclear protein extracted from MCF7-derived mammospheres is shown. Lane 1, nuclear extracts with probe; lane 2, TA (10 μM)-treated nuclear extracts with probe; lane 3, TA (20 μM)-treated nuclear extracts with probe. (E, F) The IL-6 concentration in both whole-cell lysate (E, western blotting) and cell-culture supernatant of MCF7-M (F, ELISA) was higher than that exhibited by the MCF7 cells, which was decreased in response to TA treatment (10 μM). Representative western blots with quantitative analyses are shown (A-C, E). The data shown are the mean ± SEM of three independent experiments. *$P < 0.05$ vs. others; #$P < 0.05$ vs. 10 μM of TA.

expression of E-cadherin, CK18, N-cadherin and fibronectin.

TGFβ treatment was furthermore shown to promote mammosphere formation and growth, indicated by an observed increase in both MFE and the average mammosphere diameter (**Figure 4E**, **4F**). TA treatment significantly reduced both the number and size of TGFβ-induced mammospheres (**Figures 4E**, **4F**, S3, S4). Consistent with this result, TGFβ increased $CD44^{high}/CD24^{low}$ ratio in MCF7 and T47D cells, which was inhibited by TA (**Figure 4G**). These data indicate TA inhibits TGFβ-induced CSC formation, which can be mediated by an amelioration of EMT of breast cancer cells.

TA reduces the TGFβ-induced NF-κB pathway activation in the MCF7 cells

Given the crucial role of NF-κB signaling and TGFβ activity in breast CSC formation, the effect of TA on TGFβ-induced NF-κB signaling was assessed. TGFβ treatment increased the nuclear translocation of p65, as well as the phosphorylation levels of both IκBα and IKK (**Figure 5A-C**). In addition, treatment of MCF7 cells with *p65* siRNA or PDTC alleviated the observed TGFβ-induced EMT (**Figure 5D**, **5E**). TA significantly alleviated TGFβ-induced activation of NF-κB signaling (**Figure 5A-C**). Collectively, these results suggest that the NF-κB pathway plays a key role in TGFβ-induced EMT in breast cancer, and effect of TA on TGFβ-induced CSC formation is mediated by an inhibition of NF-κB signaling.

TA reduces the tumor growth and stemness markers in a mouse xenograft model

Based on the aforementioned role of TA in the formation of CSCs and NF-κB signaling, we further evaluated the effect of TA on tumor growth in a mouse xenograft model of breast cancer. As shown in **Figure 6A**, when tumors reached a volume of 70-100 mm^3 after SQ implantation of MCF7 cells, tumor-bearing mice were treated with TGFβ (40 ng/kg) three times/wk facilitate tumor growth with or without TA (2 mg/kg) twice/wk (on alternative days to the TGFβ injection) for 4 weeks. Tumor growth was significantly accelerated by TGFβ injection despite comparable body weight with other groups (**Figure 6B**). TA treatment significantly inhibited tumor growth, as indicated by a reduction in both the weight and volume of the observed tumor mass (**Figure 6C**). On day 31 after treatment initiation, the tumors resected from in TGFβ + TA group were significantly smaller than those exhibited by TGFβ group. Specifically, the tumor weights observed in the Vehicle, TGFβ, and TGFβ + TA groups were 73.58 ± 17.21, 308 ± 53.04, and 113.7 ± 7.041 mg, respectively ($P < 0.01$ by ANOVA). Similarly, the tumor volumes observed in each group were 141.2 ± 44.49, 429.5 ± 61.97, and 126.1 ± 25.64 mm^3, respectively ($P < 0.01$ by ANOVA) (**Figure 6D**).

To demonstrate the effect of TA on cancer stemness and NF-κB signaling in-vivo, we performed the IHC and western blotting of resected tumor tissue. Abundant expression of ALDH1 and CD44, as well as reduced CD24 levels and IKK activation were observed in the breast-tumor tissues of TGFβ group compared to the control group; which were attenuated in TGFβ + TA group (**Figure 6E-G**).

Discussion

The present study demonstrated that TA treatment exerts an inhibitory effect on the formation and growth of breast CSCs *in vitro* by inhibiting NF-κB signaling, as indicated by the

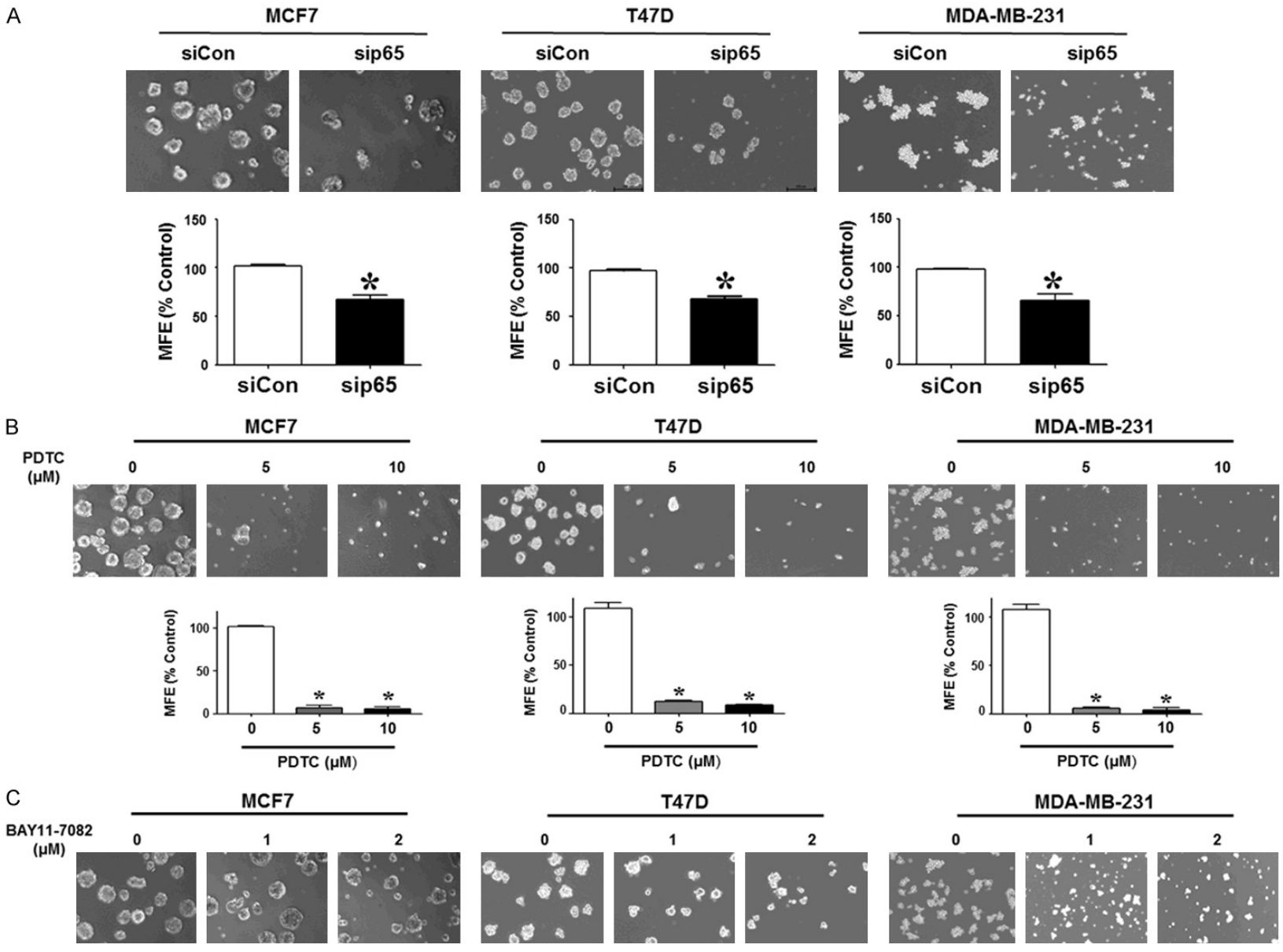
A
MCF7
T47D
MDA-MB-231
siCon
sip65
MFE (% Control)
150
100
50
0
*
B
PDTC (μM)
0
5
10
PDTC (μM)
C
BAY11-7082 (μM)
0
1
2

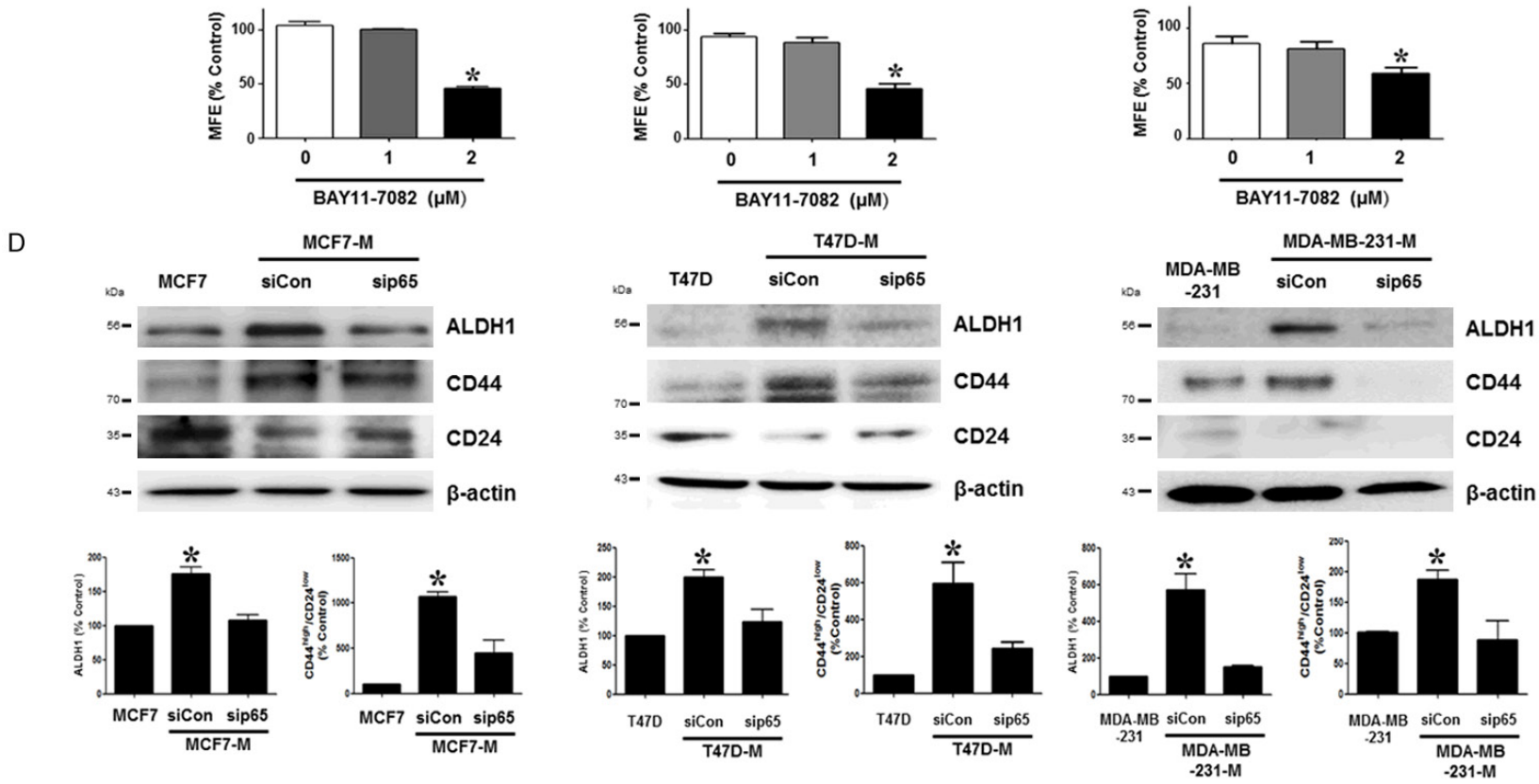

Figure 3. Blocking NF-κB signaling inhibits the formation of breast CSCs. (A-C) NF-κB signaling inhibition, induced via *p65* siRNA transfection (A), or via treatment with either a NF-κB pathway-specific (PDTC; 5 and 10 μM, B) or IKK-specific inhibitor, (Bay11-7082; 2 μM, C), resulted in a significant decrease in the MFE in MCF7, T47D, and MDA-MB-231 cells. Magnification, × 200. (D) siRNA-induced silencing of *p65* decreased the expression of CSC markers, (e.g. ALDH1 expression, $CD44^{high}/CD24^{low}$ ratio) in MCF7-M, T47D-M, and MDA-MB-231-M. A representative images of mammosphere (A-C) and western blot with quantitation bar (D) are shown. The data shown are the mean ± SEM of three independent experiments. *P < 0.05 vs. others.

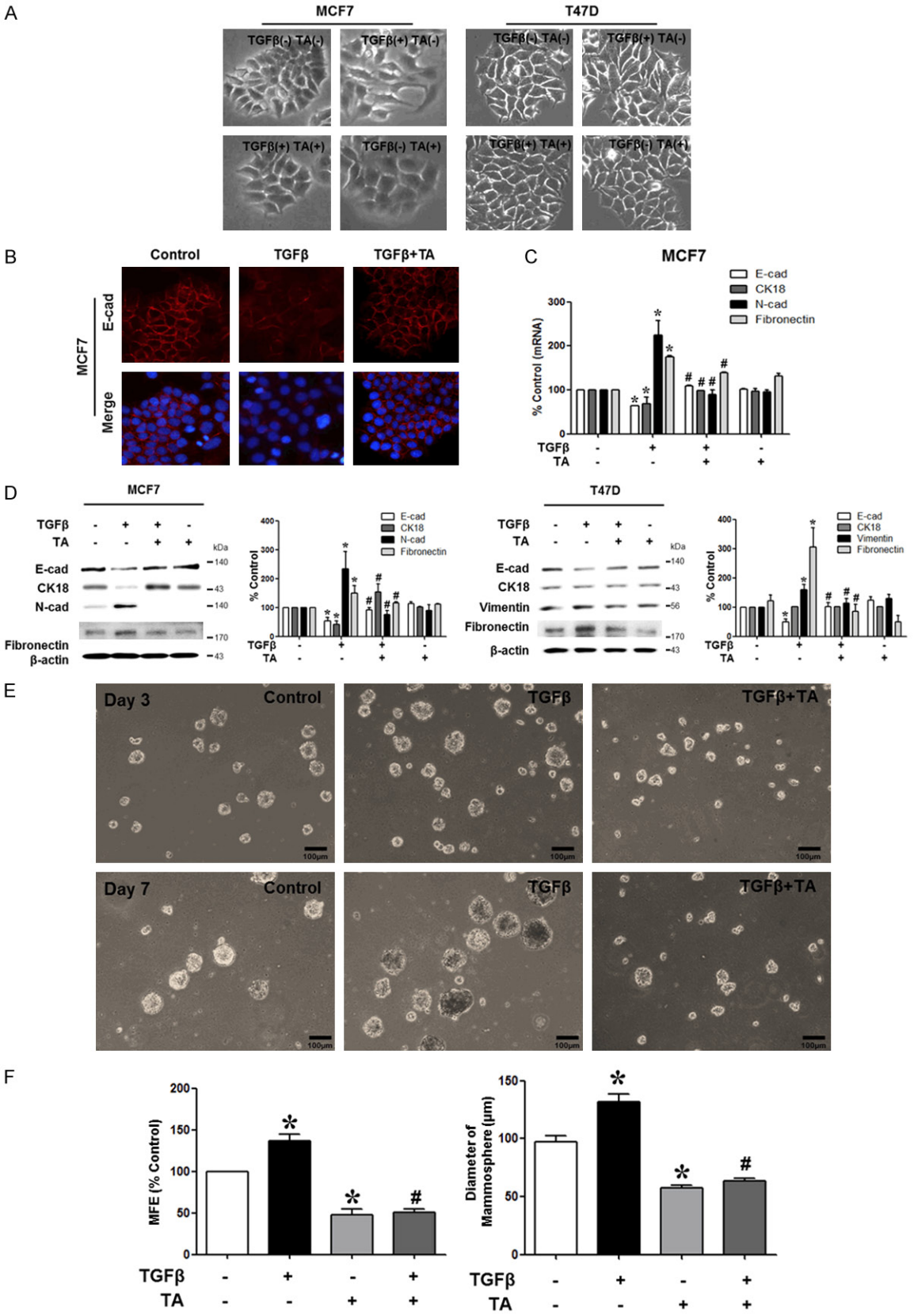
A
MCF7
T47D
TGFβ(-) TA(-)
TGFβ(+) TA(-)
TGFβ(+) TA(+)
TGFβ(-) TA(+)
B
Control
TGFβ
TGFβ+TA
MCF7
E-cad
Merge
C
MCF7
E-cad
CK18
N-cad
Fibronectin
% Control (mRNA)
TGFβ
TA
D
MCF7
T47D
TGFβ
TA
kDa
E-cad
CK18
N-cad
Fibronectin
β-actin
Vimentin
% Control
E-cad
CK18
N-cad
Fibronectin
Vimentin
E
Day 3
Day 7
Control
TGFβ
TGFβ+TA
100μm
F
MFE (% Control)
Diameter of Mammosphere (μm)
TGFβ
TA

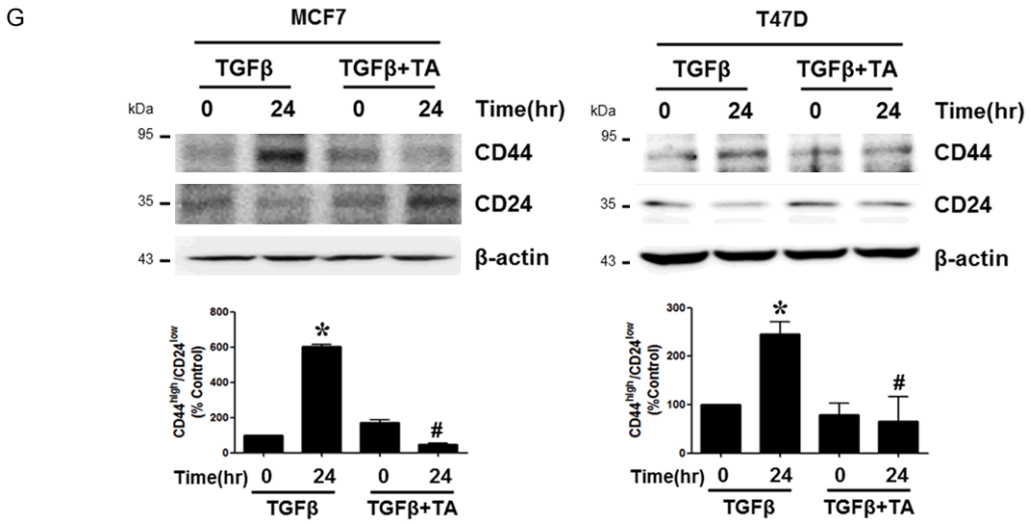

Figure 4. TA reduces TGFβ-induced EMT and cancer stem cell properties in MCF7 and T47D cells. (A) TGFβ treatment (10 ng/ml) induced morphological changes in the MCF7 and T47D cells, (including a loss of cell contact and elongation), which was ameliorated by treatment with TA (10 μM). (B) TA treatment alleviated the TGFβ-induced decrease and cytoplasmic localization of E-cadherin (red) in the MCF7 cells. Representative photos of cell morphology and immunofluorescent staining are shown, Nuclei are stained with DAPI (blue). Magnification × 200. (C, D) Real-time PCR (C) and western blot analysis (D) (with quantitation bar) showing the TGFβ-induced EMT shown as the decreased expression of the epithelial cell marker, E-cadherin (E-cad), cytokeratin 18 (CK18), and increased expression of the mesenchymal marker, N-cadherin (N-cad), Vimentin and Fibronectin. (E, F) TGFβ treatment enhanced mammosphere formation on days 3 and 7 after the initiation of treatment. TA treatment (10 μM) subsequently reduced both the MFE and average mammosphere size. Representative photos of mammosphere are shown (E). Scale bar = 100 μm. (G) TA treatment ameliorated the TGFβ-induced alteration in $CD44^{high}/CD24^{low}$ expression. β-actin was used as a loading control. The data shown represent the mean ± SEM of four independent experiments. *P < 0.05 vs. control; #P < 0.05 vs. TGFβ.

observed reduction in the rate of nuclear p65 translocation, and by the increased and decreased production of IκBα and IL-6, respectively. TA treatment also prevented TGFβ-induced EMT and NF-κB-pathway activation, and thereby prevented the TGFβ-induced increase in CSC formation and stemness-marker expression by breast-cancer cells. Importantly, TA treatment was also shown to decrease tumor growth and cancer stemness-marker expression in xenograft tumor transplant model in Balb/c nude mice.

It is already known that TA has anti-proliferative effect on cancer cells with an induction of apoptosis [27-30]. In addition to its well-known anti-oxidant effect [25], TA is reported to suppress the activity of tyrosine kinase and to serve as anti-angiogenic factor of breast cancer [31]. A recent study showed that TA treatment was sufficient to inhibit EGFR/STAT3 activation and enhance p38/STAT1 signaling, and thereby cause G1 arrest and intrinsic apoptosis in breast cancer cells [29, 30]. However, despite several studies demonstrating the potential anti-cancer effect of TA, no data is currently available detailing its effect on CSCs. Thus, the present study is the first to demonstrate an inhibitory effect of mammosphere formation, and by TA on the formation and growth of breast CSCs, as indicated by the decrease in mammosphere diameter, and number of constituent mammosphere cells. These effects were furthermore maintained during secondary and tertiary mammosphere assays. The low MFE achieved during TA treatment was associated with a low reduction in the expression of stem-cell markers, including ALDH1 activity and the $CD44^{high}/CD24^{low}$ ratio. This result is particularly interesting given that the dose of TA administered in the present study was less than half that used in previous studies [29]. The concentrations of TA used in the present study were 10 and 20 μM, as these were the doses determined via the preliminary experiment to not affect the viability or proliferation of normal breast cells, as compared to the higher concentrations (e.g. 60 μM) used by previous studies

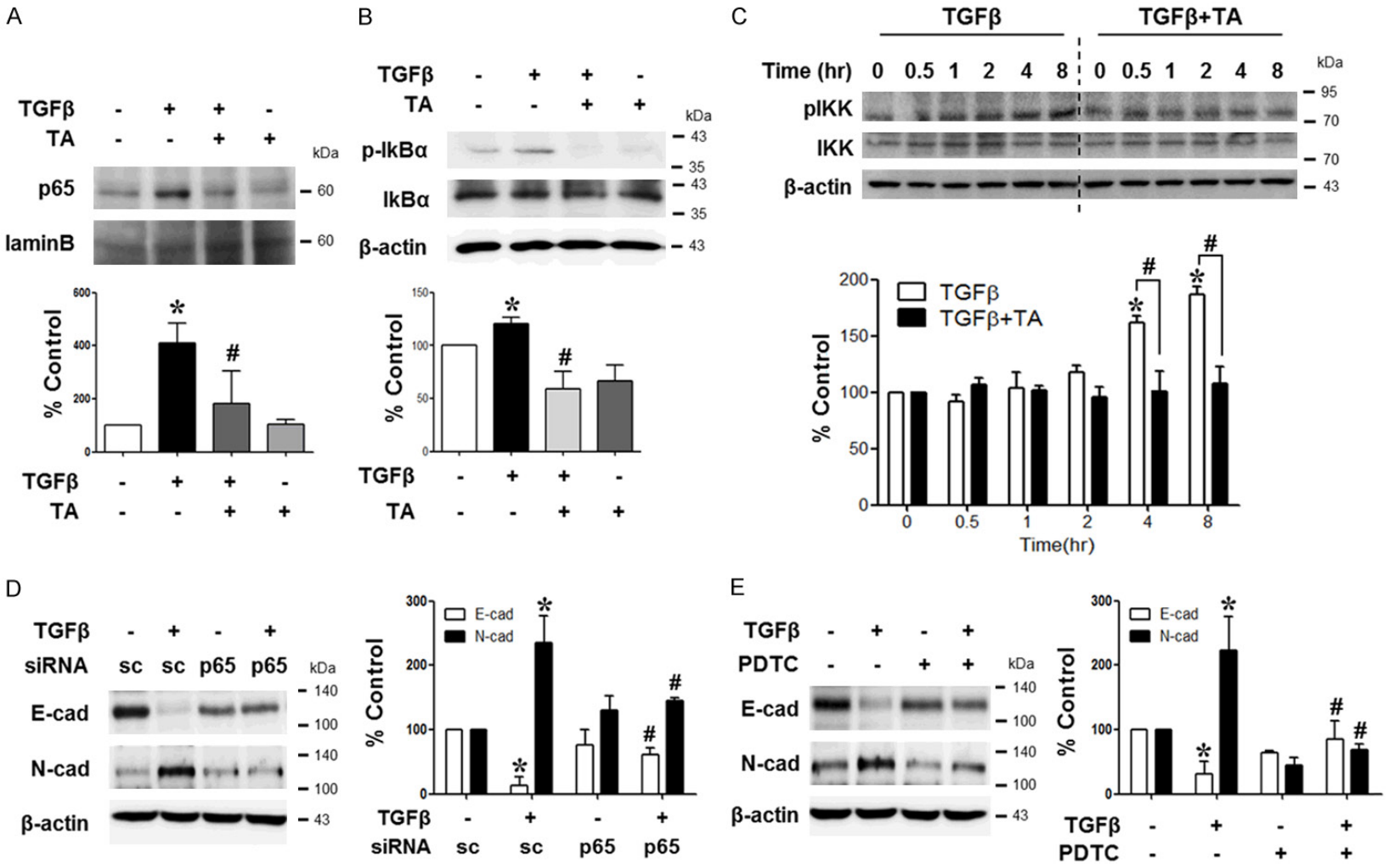

Figure 5. TA reduces the TGFβ-induced NF-kB pathway activation in MCF7 cells. (A-C) TGFβ treatment enhanced the nuclear translocation of p65 (2 h), the phosphorylation of IκBα (30 min) and IKK (4 h), all of which were inhibited upon treatment with TA. (n = 4). (D, E) *p65* siRNA transfection and/or PDTC ameliorated the TGFβ-induced alteration of E-cadherin and N-cadherin expression (n = 3). Representative western blots are shown with quantitation bars (A-E). β-actin was used as a loading control. The data shown represent the mean ± SEM. *P < 0.05 vs. control; #P < 0.05 vs. TGFβ.

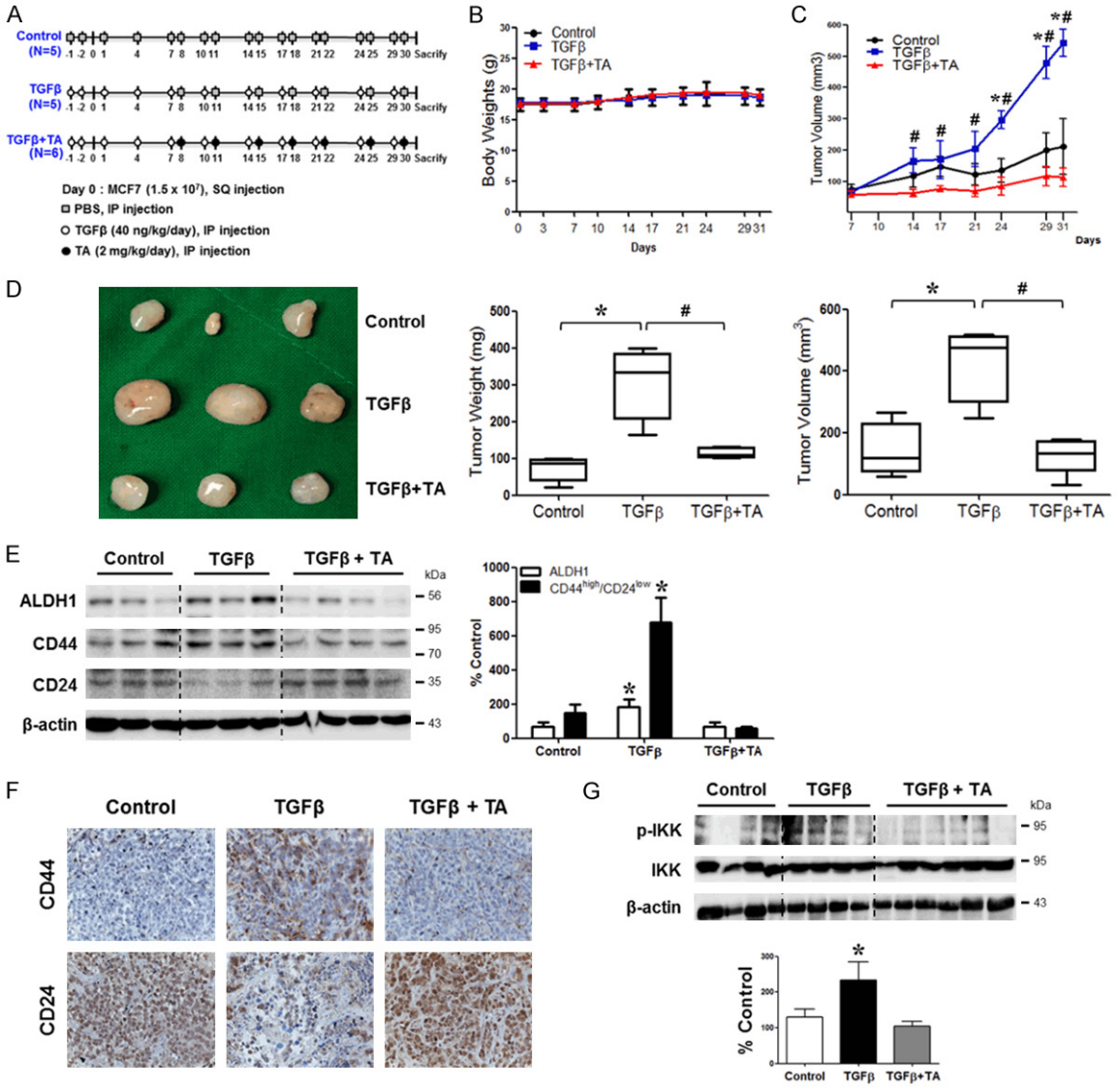

Figure 6. TA reduces the tumor growth and markers of stemness in a mouse xenograft model. (A) Schematic protocol of in-vivo experiment. MCF7 breast cancer cell lines (1.5×10^7 cells) were injected into Balb/c nu-nu mice via subcutaneous route. Phosphate buffered saline, TGFβ and TA were injected intraperitoneally at the time indicated. The mice were sacrificed on day 31. (B-D) The body weights of the mice throughout the study were comparable among the treatment groups. TGFβ administration resulted in a significant increase in tumor volume compared to control group. Tumor weight and volume were found to be lower in the TGFβ + TA compared to the TGFβ group. *P < 0.05 vs. control; #P < 0.05 vs. TGFβ + TA. (E, F) The expression of ALDH1 and $CD44^{high}/CD24^{low}$ in tumor tissues was enhanced in the TGFβ group, as assessed via western blot analysis (E) and immunohistochemistry (F; magnification × 400). These effects were rescued by TA treatment. (G) TGFβ injection resulted in an increased level of IKK phosphorylation in the tumor tissues, which was inhibited by treatment with TA. Representative western blots are shown with quantitation bars (E, G). *P < 0.05 vs. others.

to demonstrate the anti-proliferative and pro-apoptotic effects of TA in MCF7 cells [30]. Furthermore, treatment with paclitaxel, which is the most commonly prescribed medicine for breast cancer, did not inhibit mammosphere formation at a concentration of 5 nM, which was the maximum concentration shown to not impact the viability of normal breast cells (Figure S2). These findings are consistent with clinical data demonstrating the ineffectiveness of paclitaxel treatment to prevent chemo-resistance or metastasis [40, 41].

One of the potential mechanisms by which TA prevents breast CSC formation is the inhibition of NF-κB signaling. Previous studies have dem-

onstrated that NF-κB and its target genes are upregulated in the majority of cancer types, including breast cancer [13, 36]. Once activated, the NF-κB pathway regulates a wide variety of target genes to support cancer-cell survival by inducing cell proliferation, inflammation, and the formation of a favorable tumor microenvironment. In the present study, increased p65 expression, and decreased IκB production, altered rates of nuclear p65 translocation, and elevated IL-6 production were all observed in the mammospheres derived from two luminal breast cancer cell lines (MCF7 and T47D cells) and triple-negative breast cancer cell line (MDA-MB-231 cells), consistent with enhanced NF-κB signaling. Secreted IL-6 is known to be an important CSC survival factor, and similarly, high levels of circulating IL-6 are correlated with poor patient prognosis in breast cancer [42]. Inhibition of the NF-κB pathway via IKKα upregulation has been previously shown to lead to a decrease in the self-renewal and senescence of breast CSCs [14]. In addition to its role in CSC formation and expansion, NF-κB signaling has also been established to contribute to the invasiveness and metastatic characteristics of CSCs [13, 14], often via an induced EMT. The present study confirmed that the NF-κB pathway plays a key role in mammosphere formation, and the induction of EMT in breast-cancer cells. Inhibiting NF-κB activation via *p65* gene silencing, and preventing nuclear translocation of p65 (using PDTC) or IkB phosphorylation (using BAY 11-7082) all reduced the exhibited MFE, ALDH1 activity, and CD44/CD24 ratio. Importantly, TA reduced the levels of nuclear p65 protein and NF-κB DNA binding activity, and inhibited the phosphorylation of both IKK and IκBα, thereby reducing the production of IL-6.

Another important finding of the present study was that TGFβ treatment promoted the expression of stemness markers by breast cancer cells, significantly increased mammosphere formation and growth, and increased the exhibited $CD44^{high}/CD24^{low}$ ratio. TGFβ treatment also induced the EMT of MCF7 and T47D cells, as evidenced by their altered morphology and expression of epithelial and mesenchymal cell markers. TGFβ is well known to induce EMT, as required for cancer cells to acquire their characteristic motile and invasive phenotype [43]. TGFβ-induced EMT observed in the present study occurred via the activation of NF-κB signaling, since it was able to be prevented by the inhibition of *p65* expression and/or nuclear p65 translocation in the MCF7 cells. Furthermore, exogenous TGFβ administration in the mouse xenograft model used in the present study was shown to promote tumor growth, which was again accompanied by increased IKK phosphorylation, and by the elevated expression of stemness markers such as ALDH1 and $CD44^{high}/CD24^{low}$. A recent study similarly detected the evidence of an induced EMT and CD44 upregulation, as well as ERK/NF-κB/Snail pathway activation in a mouse xenograft model of breast cancer [20]. Arsura *et al.* also demonstrated NF-κB signaling to be a downstream target of TGFβ signaling [44], and showed that TGFβ treatment was sufficient to cause a transient upregulation of NF-κB activity via activation of the TAK1/IKK complex, leading to the inhibition of AP-1 complex activity in liver cancer [45].

In summary, the present study showed that TA treatment alleviated the formation and growth of breast CSCs, and prevented them from undergoing an EMT, via the induced inhibition of NF-κB signaling. These data strongly support TA as a promising therapeutic agent for the treatment of breast cancer, either alone, or in combination with other therapeutic strategies to inhibit cancer cell metastasis and prevent chemo-resistance.

Acknowledgements

This work was supported by the Korean Health Technology R&D Project, Ministry of Health & Welfare, Republic of Korea (HI12C0050) and the National Research Foundation of Korea (NRF) grant funded by the Korea government (MSIP) (NRF-2017R1A6A3A11034413; NRF-2019R1I1A1A01055061), the RP-Grant 2016 of Ewha Womans University (1-2016-0948-001-1), and intramural research promotion grants from Ewha Womans University School of Medicine (1-2014-0665-001-1).

Disclosure of conflict of interest

None.

Address correspondence to: Dr. Duk-Hee Kang, Department of Internal Medicine, College of Medicine, Ewha Womans University, Seoul 07804, Republic of

Korea; Ewha Medical Research Center, College of Medicine, Ewha Womans University, Seoul 07804, Republic of Korea. Tel: 82-2-6986-1637; E-mail: dhkang@ewha.ac.kr

References

[1] DeSantis C, Howlader N, Cronin KA and Jemal A. Breast cancer incidence rates in U.S. women are no longer declining. Cancer Epidemiol Biomarkers Prev 2011; 20: 733-739.

[2] Kakarala M and Wicha MS. Implications of the cancer stem-cell hypothesis for breast cancer prevention and therapy. J Clin Oncol 2008; 26: 2813-2820.

[3] Hou ZJ, Luo X, Zhang W, Peng F, Cui B, Wu SJ, Zheng FM, Xu J, Xu LZ, Long ZJ, Wang XT, Li GH, Wan XY, Yang YL and Liu Q. Flubendazole, FDA-approved anthelmintic, targets breast cancer stem-like cells. Oncotarget 2015; 6: 6326-6340.

[4] Ailles LE and Weissman IL. Cancer stem cells in solid tumors. Curr Opin Biotechnol 2007; 18: 460-466.

[5] Reya T, Morrison SJ, Clarke MF and Weissman IL. Stem cells, cancer, and cancer stem cells. Nature 2001; 414: 105-111.

[6] O'Connor ML, Xiang D, Shigdar S, Macdonald J, Li Y, Wang T, Pu C, Wang Z, Qiao L and Duan W. Cancer stem cells: a contentious hypothesis now moving forward. Cancer Lett 2014; 344: 180-187.

[7] Hambardzumyan D, Squatrito M and Holland EC. Radiation resistance and stem-like cells in brain tumors. Cancer Cell 2006; 10: 454-456.

[8] Ginestier C, Hur MH, Charafe-Jauffret E, Monville F, Dutcher J, Brown M, Jacquemier J, Viens P, Kleer CG, Liu S, Schott A, Hayes D, Birnbaum D, Wicha MS and Dontu G. ALDH1 is a marker of normal and malignant human mammary stem cells and a predictor of poor clinical outcome. Cell Stem Cell 2007; 1: 555-567.

[9] Gupta PB, Onder TT, Jiang G, Tao K, Kuperwasser C, Weinberg RA and Lander ES. Identification of selective inhibitors of cancer stem cells by high-throughput screening. Cell 2009; 138: 645-659.

[10] Creighton CJ, Li X, Landis M, Dixon JM, Neumeister VM, Sjolund A, Rimm DL, Wong H, Rodriguez A, Herschkowitz JI, Fan C, Zhang X, He X, Pavlick A, Gutierrez MC, Renshaw L, Larionov AA, Faratian D, Hilsenbeck SG, Perou CM, Lewis MT, Rosen JM and Chang JC. Residual breast cancers after conventional therapy display mesenchymal as well as tumor-initiating features. Proc Natl Acad Sci U S A 2009; 106: 13820-13825.

[11] DiDonato JA, Mercurio F and Karin M. NF-kappaB and the link between inflammation and cancer. Immunol Rev 2012; 246: 379-400.

[12] Perkins ND. The diverse and complex roles of NF-kappaB subunits in cancer. Nat Rev Cancer 2012; 12: 121-132.

[13] Liu M, Sakamaki T, Casimiro MC, Willmarth NE, Quong AA, Ju X, Ojeifo J, Jiao X, Yeow WS, Katiyar S, Shirley LA, Joyce D, Lisanti MP, Albanese C and Pestell RG. The canonical NF-kappaB pathway governs mammary tumorigenesis in transgenic mice and tumor stem cell expansion. Cancer Res 2010; 70: 10464-10473.

[14] Cao Y, Luo JL and Karin M. IkappaB kinase alpha kinase activity is required for self-renewal of ErbB2/Her2-transformed mammary tumor-initiating cells. Proc Natl Acad Sci U S A 2007; 104: 15852-15857.

[15] Christiansen JJ and Rajasekaran AK. Reassessing epithelial to mesenchymal transition as a prerequisite for carcinoma invasion and metastasis. Cancer Res 2006; 66: 8319-8326.

[16] Bill R and Christofori G. The relevance of EMT in breast cancer metastasis: correlation or causality? FEBS Lett 2015; 589: 1577-1587.

[17] Morel AP, Lievre M, Thomas C, Hinkal G, Ansieau S and Puisieux A. Generation of breast cancer stem cells through epithelial-mesenchymal transition. PLoS One 2008; 3: e2888.

[18] Lamouille S, Xu J and Derynck R. Molecular mechanisms of epithelial-mesenchymal transition. Nat Rev Mol Cell Biol 2014; 15: 178-196.

[19] Gonzalez DM and Medici D. Signaling mechanisms of the epithelial-mesenchymal transition. Sci Signal 2014; 7: re8.

[20] Han D, Wu G, Chang C, Zhu F, Xiao Y, Li Q, Zhang T and Zhang L. Disulfiram inhibits TGF-beta-induced epithelial-mesenchymal transition and stem-like features in breast cancer via ERK/NF-kappaB/Snail pathway. Oncotarget 2015; 6: 40907-40919.

[21] Mani SA, Guo W, Liao MJ, Eaton EN, Ayyanan A, Zhou AY, Brooks M, Reinhard F, Zhang CC, Shipitsin M, Campbell LL, Polyak K, Brisken C, Yang J and Weinberg RA. The epithelial-mesenchymal transition generates cells with properties of stem cells. Cell 2008; 133: 704-715.

[22] Singh A and Settleman J. EMT, cancer stem cells and drug resistance: an emerging axis of evil in the war on cancer. Oncogene 2010; 29: 4741-4751.

[23] May CD, Sphyris N, Evans KW, Werden SJ, Guo W and Mani SA. Epithelial-mesenchymal transition and cancer stem cells: a dangerously dynamic duo in breast cancer progression. Breast Cancer Res 2011; 13: 202.

[24] Choi HS, Kim DA, Chung H, Park IH, Kim BH, Oh ES and Kang DH. Screening of breast cancer stem cell inhibitors using a protein kinase inhibitor library. Cancer Cell Int 2017; 17: 25.

[25] Cai Y, Luo Q, Sun M and Corke H. Antioxidant activity and phenolic compounds of 112 traditional Chinese medicinal plants associated with anticancer. Life Sci 2004; 74: 2157-2184.

[26] Andrade RG Jr, Dalvi LT, Silva JM Jr, Lopes GK, Alonso A and Hermes-Lima M. The antioxidant effect of tannic acid on the in vitro copper-mediated formation of free radicals. Arch Biochem Biophys 2005; 437: 1-9.

[27] Cosan D, Soyocak A, Basaran A, Degirmenci I and Gunes HV. The effects of resveratrol and tannic acid on apoptosis in colon adenocarcinoma cell line. Saudi Med J 2009; 30: 191-195.

[28] Booth BW, Inskeep BD, Shah H, Park JP, Hay EJ and Burg KJ. Tannic acid preferentially targets estrogen receptor-positive breast cancer. Int J Breast Cancer 2013; 2013: 369609.

[29] Darvin P, Baeg SJ, Joung YH, Sp N, Kang DY, Byun HJ, Park JU and Yang YM. Tannic acid inhibits the Jak2/STAT3 pathway and induces G1/S arrest and mitochondrial apoptosis in YD-38 gingival cancer cells. Int J Oncol 2015; 47: 1111-1120.

[30] Darvin P, Joung YH, Kang DY, Sp N, Byun HJ, Hwang TS, Sasidharakurup H, Lee CH, Cho KH, Park KD, Lee HK and Yang YM. Tannic acid inhibits EGFR/STAT1/3 and enhances p38/STAT1 signalling axis in breast cancer cells. J Cell Mol Med 2017; 21: 720-734.

[31] Chen X, Beutler JA, McCloud TG, Loehfelm A, Yang L, Dong HF, Chertov OY, Salcedo R, Oppenheim JJ and Howard OM. Tannic acid is an inhibitor of CXCL12 (SDF-1alpha)/CXCR4 with antiangiogenic activity. Clin Cancer Res 2003; 9: 3115-3123.

[32] Weaver BA. How taxol/paclitaxel kills cancer cells. Mol Biol Cell 2014; 25: 2677-2681.

[33] Jang YH, Shin HS, Sun Choi H, Ryu ES, Jin Kim M, Ki Min S, Lee JH, Kook Lee H, Kim KH and Kang DH. Effects of dexamethasone on the TGF-beta1-induced epithelial-to-mesenchymal transition in human peritoneal mesothelial cells. Lab Invest 2013; 93: 194-206.

[34] Patel NJ, Karuturi R, Al-Horani RA, Baranwal S, Patel J, Desai UR and Patel BB. Synthetic, nonsaccharide, glycosaminoglycan mimetics selectively target colon cancer stem cells. ACS Chem Biol 2014; 9: 1826-1833.

[35] Shostak K and Chariot A. NF-kappaB, stem cells and breast cancer: the links get stronger. Breast Cancer Res 2011; 13: 214.

[36] Hinohara K, Kobayashi S, Kanauchi H, Shimizu S, Nishioka K, Tsuji E, Tada K, Umezawa K, Mori M, Ogawa T, Inoue J, Tojo A and Gotoh N. ErbB receptor tyrosine kinase/NF-kappaB signaling controls mammosphere formation in human breast cancer. Proc Natl Acad Sci U S A 2012; 109: 6584-6589.

[37] Libermann TA and Baltimore D. Activation of interleukin-6 gene expression through the NF-kappa B transcription factor. Mol Cell Biol 1990; 10: 2327-2334.

[38] Bruna A, Greenwood W, Le Quesne J, Teschendorff A, Miranda-Saavedra D, Rueda OM, Sandoval JL, Vidakovic AT, Saadi A, Pharoah P, Stingl J and Caldas C. TGFbeta induces the formation of tumour-initiating cells in claudinlow breast cancer. Nat Commun 2012; 3: 1055.

[39] Bellomo C, Caja L and Moustakas A. Transforming growth factor beta as regulator of cancer stemness and metastasis. Br J Cancer 2016; 115: 761-769.

[40] Kajiyama H, Shibata K, Terauchi M, Yamashita M, Ino K, Nawa A and Kikkawa F. Chemoresistance to paclitaxel induces epithelial-mesenchymal transition and enhances metastatic potential for epithelial ovarian carcinoma cells. Int J Oncol 2007; 31: 277-283.

[41] DeNardo DG, Brennan DJ, Rexhepaj E, Ruffell B, Shiao SL, Madden SF, Gallagher WM, Wadhwani N, Keil SD, Junaid SA, Rugo HS, Hwang ES, Jirstrom K, West BL and Coussens LM. Leukocyte complexity predicts breast cancer survival and functionally regulates response to chemotherapy. Cancer Discov 2011; 1: 54-67.

[42] Bachelot T, Ray-Coquard I, Menetrier-Caux C, Rastkha M, Duc A and Blay JY. Prognostic value of serum levels of interleukin 6 and of serum and plasma levels of vascular endothelial growth factor in hormone-refractory metastatic breast cancer patients. Br J Cancer 2003; 88: 1721-1726.

[43] Heldin CH, Vanlandewijck M and Moustakas A. Regulation of EMT by TGFbeta in cancer. FEBS Lett 2012; 586: 1959-1970.

[44] Arsura M, FitzGerald MJ, Fausto N and Sonenshein GE. Nuclear factor-kappaB/Rel blocks transforming growth factor beta1-induced apoptosis of murine hepatocyte cell lines. Cell Growth Differ 1997; 8: 1049-1059.

[45] Arsura M, Panta GR, Bilyeu JD, Cavin LG, Sovak MA, Oliver AA, Factor V, Heuchel R, Mercurio F, Thorgeirsson SS and Sonenshein GE. Transient activation of NF-kappaB through a TAK1/IKK kinase pathway by TGF-beta1 inhibits AP-1/SMAD signaling and apoptosis: implications in liver tumor formation. Oncogene 2003; 22: 412-425.

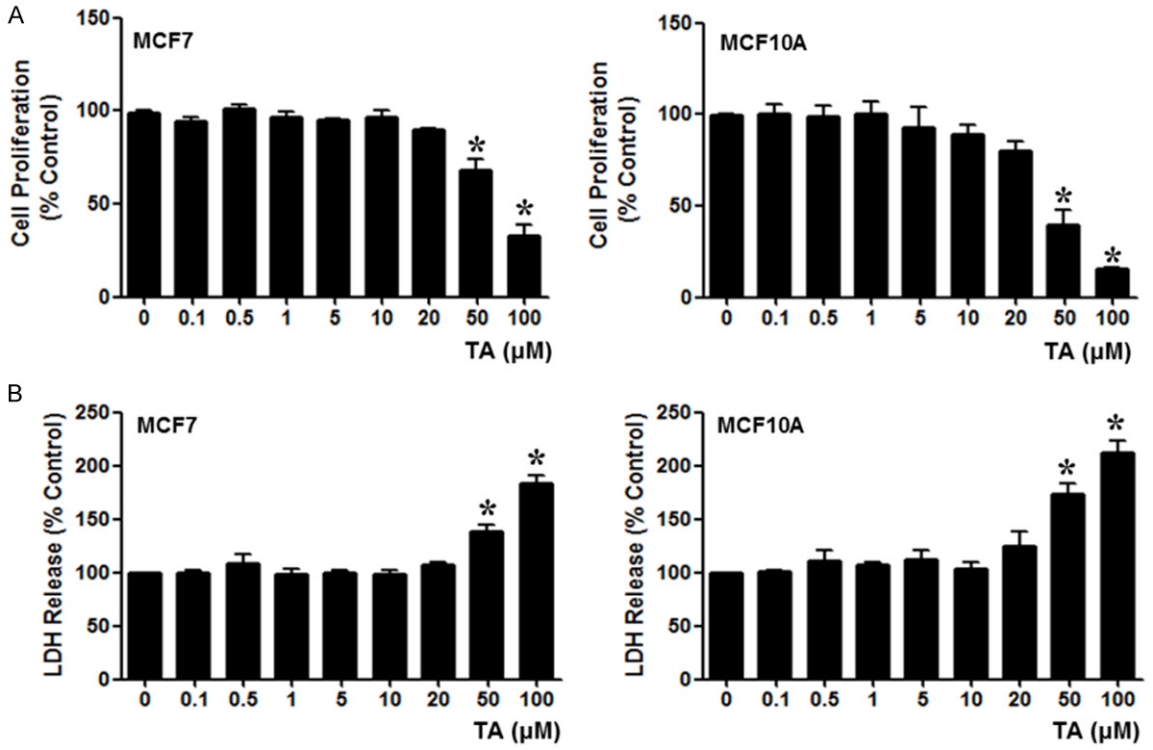

Figure S1. Effect of tannic acid (TA) on the proliferation and viability of breast cells. (A) TA inhibited cell proliferation (as assessed by MTT assay), and (B) increased the rate of LDH release, when administered at the concentrations of 50 μM or higher for 48 h in MCF7 and MCF10A cells. The data shown represent the mean ± SEM. *p < 0.05 vs. others.

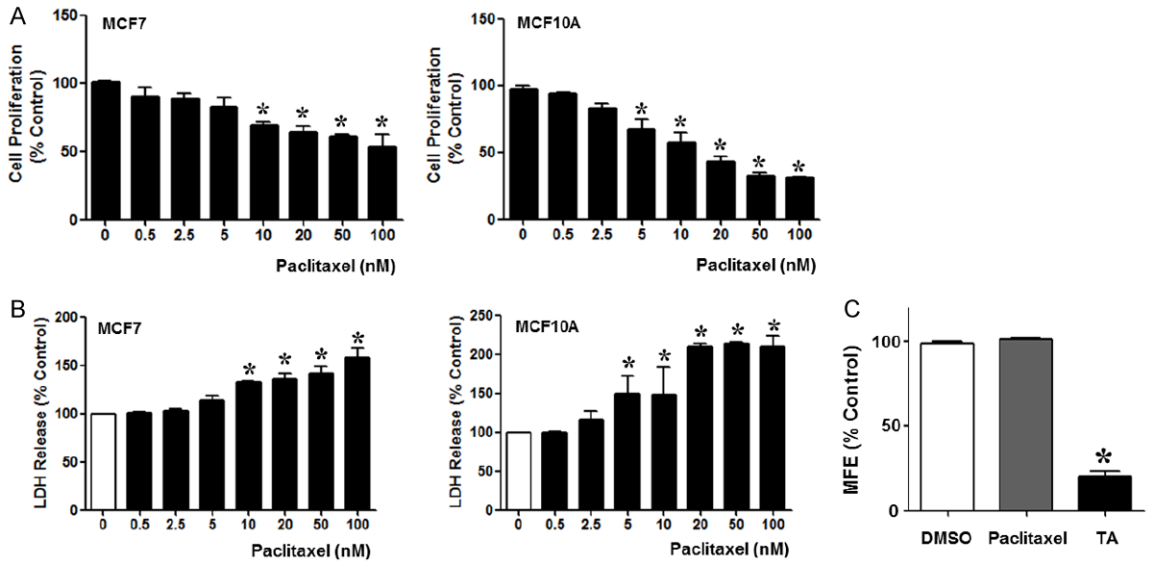

Figure S2. Effect of paclitaxel and tannic acid (TA) on the proliferation, viability and MFE of breast cells. A. Paclitaxel treatment inhibited the proliferation of MCF7 and MCF10A cells at the concentrations higher than 10 nM and 5 nM, respectively (over 48 hours), as assessed by MTT assay. B. Paclitaxel also increased the LDH release by MCF7 and MCF10A cells at the concentrations higher than 10 nM and 5 nM, respectively. C. In MCF7 cell, paclitaxel did not inhibit mammosphere formation at a concentration of 5 nM, whereas TA treatment (20 μM) significantly decreased mammosphere formation. The data shown represent the mean ± SEM. *p < 0.05 vs. others.

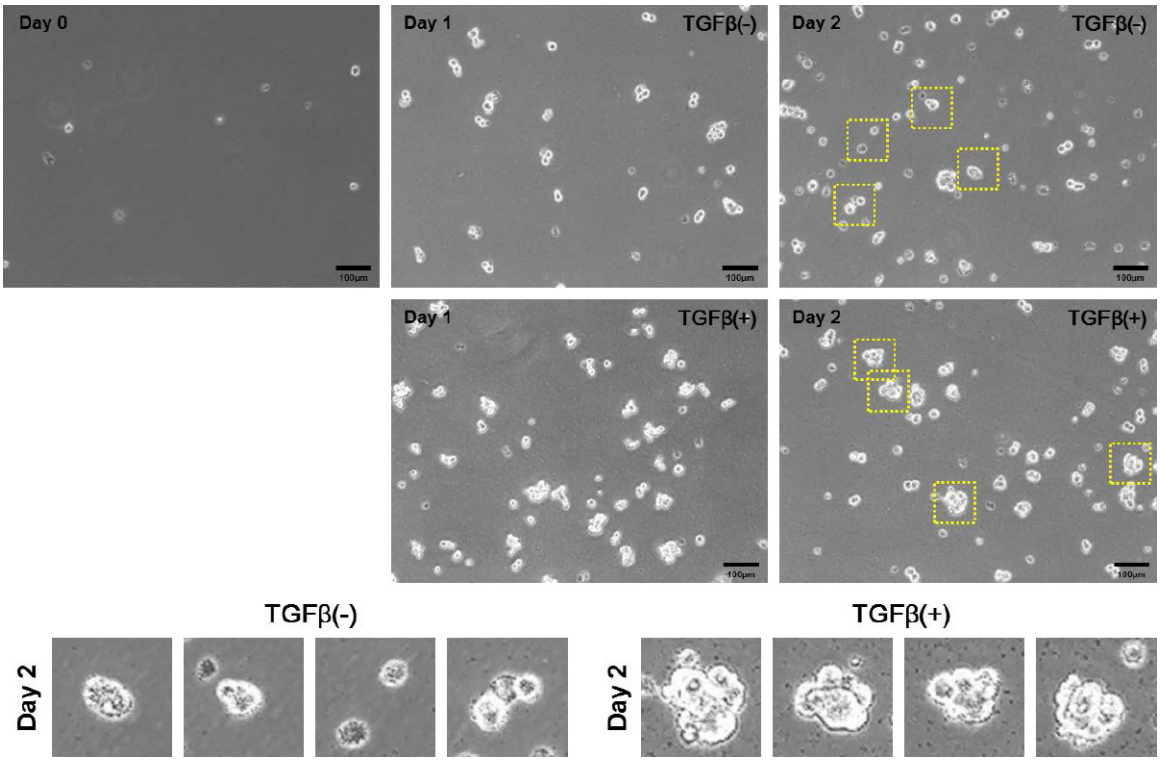

Figure S3. TGFβ enhances the mammosphere forming ability in MCF7 cells. Representative images of tumor spheres are shown. TGFβ treatment (10 ng/mL) enhanced mammosphere formation on day 2 after treatment initiation. Lower panel indicates the magnified views in the yellow boxes. Scale bar = 100 μm.

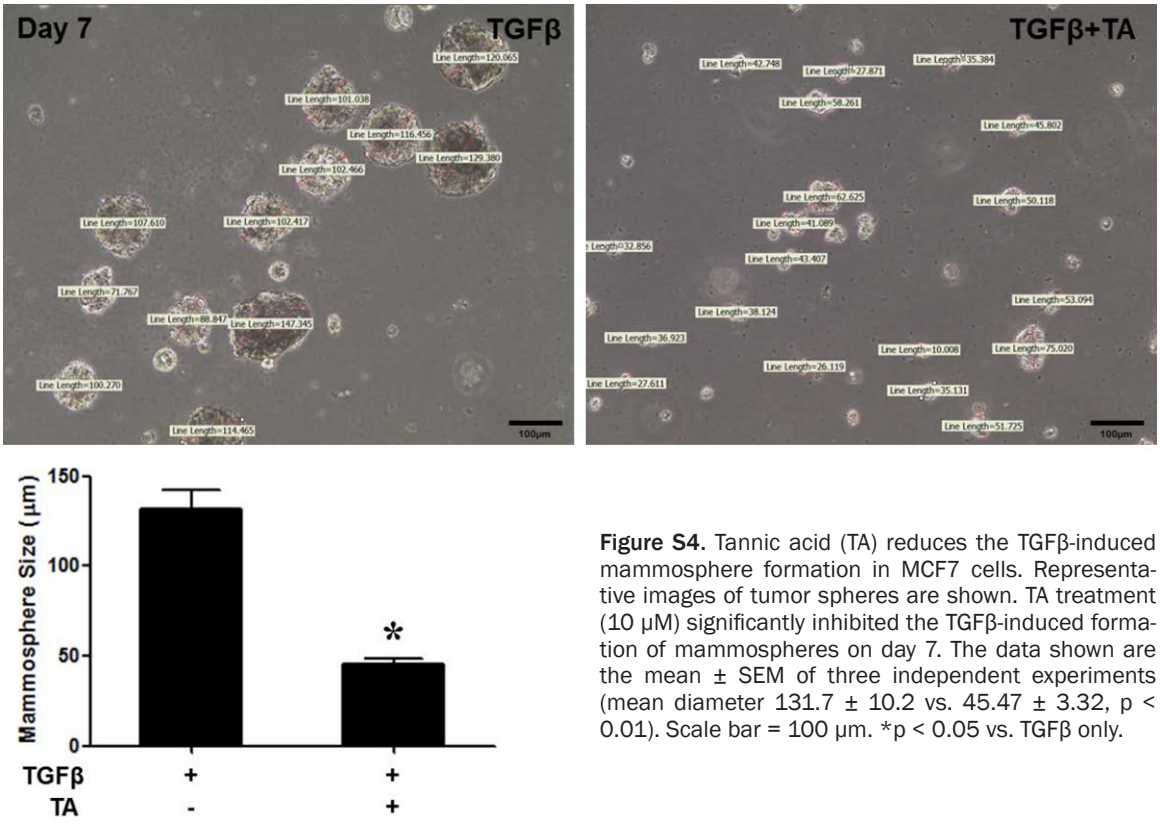

Figure S4. Tannic acid (TA) reduces the TGFβ-induced mammosphere formation in MCF7 cells. Representative images of tumor spheres are shown. TA treatment (10 μM) significantly inhibited the TGFβ-induced formation of mammospheres on day 7. The data shown are the mean ± SEM of three independent experiments (mean diameter 131.7 ± 10.2 vs. 45.47 ± 3.32, $p < 0.01$). Scale bar = 100 μm. *$p < 0.05$ vs. TGFβ only.